Chinese Chemical Letters 34 (2023) 107586

Contents lists available at ScienceDirect

Chinese Chemical Letters

journal homepage: www.elsevier.com/locate/cclet

Monitoring the pH fluctuation of lysosome under cell stress using a near-infrared ratiometric fluorescent probe

Lijuan Gui[a,1], Kaizhen Wang[a,1], Yuxin Wang[a], Jun Yan[a], Xian Liu[b], Jingxuan Guo[a], Ji Liu[a], Dawei Deng[a,*], Haiyan Chen[a,*], Zhenwei Yuan[a,*]

[a] Department of Biomedical Engineering, School of Engineering, China Pharmaceutical University, Nanjing 210009, China
[b] Department of Health Technology and Informatics, Faculty of Health and Social Sciences, The Hong Kong Polytechnic University, Hong Kong, China

ARTICLE INFO

Article history:
Received 14 March 2022
Revised 1 June 2022
Accepted 5 June 2022
Available online 10 June 2022

Keywords:
APAP-induced liver injury
Ratiometric fluorescent probe
Lysosomal pH
Cell stress

ABSTRACT

Cell stress responses are associated with numerous diseases including diabetes, neurodegenerative diseases, and cancer. Several events occur under cell stress, in which, are protein expression and organelle-specific pH fluctuation. To understand the lysosomal pH variation under cell stress, a novel NIR ratiometric pH-responsive fluorescent probe (BLT) with lysosomes localization capability was developed. The quinoline ring of BLT combined with hydrogen ion which triggered the rearrangement of π electrons conjugated at low pH medium, meanwhile, the absorption and fluorescent spectra of BLT showed a red-shifts, which gived a ratiometric signal. Moreover, the probe BLT with a suitable pK_a value has the potential to discern changes in lysosomal pH, either induced by heat stress or oxidative stress or acetaminophen-induced (APAP) injury stress. Importantly, this ratiometric fluorescent probe innovatively tracks pH changes in lysosome in APAP-induced liver injury in live cells, mice, and zebrafish. The probe BLT as a novel fluorescent probe possesses important value for exploring lysosomal-associated physiological varieties of drug-induced hepatotoxicity.

Once cell stress occurs, the foremost action is to defend that promotes cell survival [1]. However, when cell adaptive capability is inadequate, cell death programs are initiated. Several events occur under cell stress, in which, are protein expression and organelle-specific pH fluctuation. Organelle pH, which is critical for maintaining a stable intracellular environment, is affected by stressors. Lysosomes are compartments in cells, with a low pH of 4.0-5.5 [2–5], and the lysosomal acidic play key roles in diverse biological events [6–8]. Aberrant pH values in lysosomes can cause cell dysfunction that affects normal function and further cause myriad diseases, such as Alzheimer's disease and serious tumors [9–11]. Therefore, to understand lysosome-associated physiological events, it is essential for tracking lysosomal pH mediated by pathological stressors [12].

Fluorescence imaging technology has provided considerable value for investigating various ion metabolism, intracellular pH change and biomolecular events since its simplicity and great response sensitivity [13–15]. Especially near infrared region (NIR) fluorescence imaging (650-900 nm) showed great advantages, including excellent tissue penetration ability and minimum autofluorescence interference in biological system [15–20]. Currently, several fluorescent molecules have been explored for dynamically observing and imaging lysosomal pH (Table S1 in Supporting information). Wang's group and Feng's group reported NIR fluorescent probes using rhodamine as the fluorophore which were triggered by H^+ to open ring and emit fluorescent [18,21]. However, those off-on probes with single emission band were difficult to get accurate data because the data was easy to be influenced with variable probe concentration and environment. Fortunately, some ratiometric fluorescent probes can effectively solve these problems by measuring the values of the fluorescence intensity ratio when response occurs [22–26]. However, to date, there are a few NIR ratiometric fluorescent probes for detecting lysosomal pH changes with fluorescence wavelengths greater than 600 nm. Meanwhile, due to the range of the lysosomal pH, some existing ratiometric fluorescent probes have some limitations, such as insignificant changes in fluorescence under acidic conditions (pH 4-6) and high pK_a [22,24]. In addition, many ratiometric fluorescent probes were applied to study the varieties of lysosome pH during apoptosis stimulated by drugs such as dexamethasone, which had achieved certain application value [18,21,27-29]. However, ratiometric fluorescent

* Corresponding authors.
E-mail addresses: dengdawei@cpu.edu.cn (D. Deng), chenhaiyan@cpu.edu.cn (H. Chen), yuanzhenwei@cpu.edu.cn (Z. Yuan).
[1] These authors contributed equally to this work.

https://doi.org/10.1016/j.cclet.2022.06.009
1001-8417/

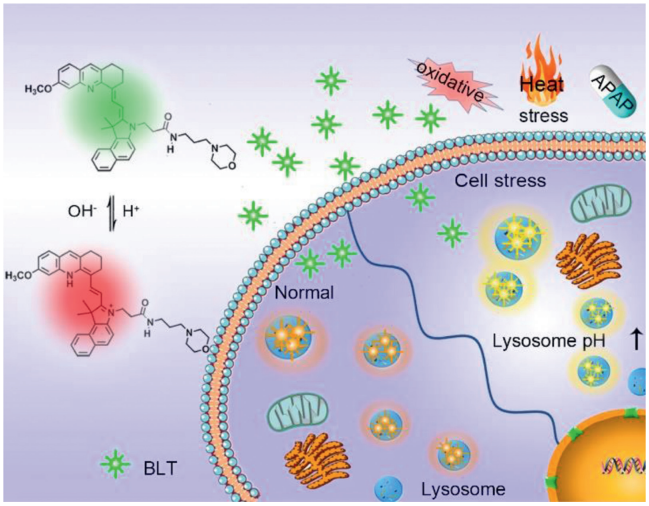

Scheme 1. Schematic diagram of BLT for the ratiometric monitoring lysosome pH under cell stress.

probes were hardly used to explore lysosome-related physiological changes upon drug-induced injury. So far, drug-induced liver injury arises widely concern, which is responsible for acute hepatotoxicity and the withdrawal of the clinical drug [30,31]. There is an urgent need to develop methods to detect drug-induced hepatotoxicity which is beneficial to improve the efficacy of drug treatment in patients [32]. Therefore, it is important to exploit a novel ratiometric NIR lysosomal pH probe possessing appropriate pK_a, favorable sensitivity to develop more biological applications.

Herein, a new lysosomal targeted pH response NIR ratiometric fluorescent probe BLT was designed to monitor pH changes in lysosome under cell stress. The probe BLT utilized a hemicyanine skeleton, *N*-(2-aminoethyl)morpholine as the lysosomal target group was selected to achieve lysosome specific staining. In acidic medium, the N atom of quinoline ring was protonated, then the rearrangement of the π electron conjugation in the fluorophore was triggered. Finally, the absorption and fluorescence spectra exhibit a distinct red-shifts. The probe BLT showed the sensitivity of pH response characteristics with ratiometric sensor. Moreover, the probe BLT with a suitable pK_a value has the potential to discern the pH changes in lysosome under cell stress induced by heat, oxidative stress or APAP-induced injury (Scheme 1). Importantly, as far as we know, this ratiometric fluorescent probe innovatively tracks changes in lysosomal pH in APAP-induced liver injury in mice and zebrafish. The novel fluorescent probe BLT is valuable for exploring lysosomal-associated physiological varieties of drug-induced hepatotoxicity.

The synthetic method of hemicyanine dyes BLT was depicted in Fig. S1 (Supporting information). The experimental compound was verified by ^{1}H NMR, ^{13}C NMR and MS (Figs. S12-S17 in Supporting information).

To explore the sensitivity to acidity, the absorption and emission spectra of BLT at various pH phosphate buffer solutions were evaluated. With the acidity of the solution system elevated, the absorption peak at 580 nm raised while the spectral band at 400-500 nm decreased, which meant that BLT has gradually transformed into an acid form (Fig. 1A). When the pH of test solution varied from 6.8 to 4, the emission peak at 670 nm of BLT ($\lambda_{ex}=580$ nm) raised dramatically with acidity of solution environment raised, and the peak at 610 nm ($\lambda_{ex}=480$ nm) concomitantly decreased (Figs. 1B and C). At the same time, we can also see the color of the solution changes with pH value (Fig. S2 in Supporting information). There are two emission bands at 610 nm and 670 nm, corresponding to products in alkaline and acid media respectively. The offset between the two emission bands was 60 nm, which avoided spectral crosstalk and was conducive to imaging living organism clearly (Fig. 1D). Because of markedly reversed pH responses of the two emission bands, BLT has the basic characteristics of ratiometric detecting pH. For instance, the fluorescence intensities ratio (I_{670}/I_{610}) revealed a 14-fold enhancement from pH 4 to pH 6, which was lysosome acidity window (pH 4-6), indicating that BLT was able to detect lysosomal pH. As shown in Figs. 1E and F, the pK_a value of BLT was measured to be 4.38 refer to Henderson-Hasselbalch formula ($\log_{10}[(I_{max}-I)/(I-I_{min})]=pH-pK_a$). BLT has a suitable p$K_a$ value and fluorescence wavelength as a lysosomal pH indicator. The quantum yields of BLT are 0.14 at pH 4 and 0.13 at pH 6 ($\lambda_{ex}=580$ nm), and 0.045 at pH 4 and 0.326 at pH 6 ($\lambda_{ex}=480$ nm).

To explore whether the polarity of the environment affected the pH detection of BLT, the absorption and fluorescence spectra of BLT in different solvents were measured. As shown in Fig. S3 (Supporting information), the absorption and fluorescence spectrum of BLT changed with different solvents, while the change of fluorescence had no obvious regularity with the polarity of the solvent. To exclude the interference of polarity under physiological conditions, the absorption and emission spectra of BLT in different ratios of 1-4 dioxane and PBS buffer solution (pH 7.4) mixtures which were better for simulating physiological conditions were performed. PBS solution as the large polar system is used to avoid the effect of pH. As depicted in Fig. S4 (Supporting information), with the increase of the polarity of the solution (the proportion of 1-4 dioxane from 10% to 90%), the absorption and fluorescence spectra of BLT changed. Fortunately, the fluctuation of fluorescence intensity ratio I_{670}/I_{610} of BLT could be ignored compared to approximately 135-fold pH response change of BLT in the physiological range (pH 4-7.4), which revealed that the polarity of the environment has little effect on the pH detection of BLT under physiological conditions. Subsequently, the absorption and emission spectra of BLT in different ratios of glycerol and methanol mixtures were tested. As the viscosity increased (glycerol from 10% to 70%), the fluorescence under both 480 nm excitation and 580 nm excitation increased, which made I_{670}/I_{610} remain stable (Fig. S5 in Supporting information). Those results showed that the viscosity did not interfere with the pH detection of BLT.

Time-dependent fluorescent intensities of BLT were also tested under the pH of solution environment at 4 and 6, which was studied by measuring the ratios of fluorescence intensity (I_{670}/I_{610}), and it was found that I_{670}/I_{610} rapidly changed and reached saturation almost immediately when BLT added into phosphate buffer solutions (Fig. 2A). The rapid response sensitivity enables BLT to track changes of pH in real time. Furthermore, the pH reversibility experiment of BLT between pH 3 and 8 was conducted. The probe exhibited excellent reversible response with fast sensitivity, which suggested that BLT had the ability for real-time monitoring in live cell (Fig. 2B).

After that, in order to explore whether pH is the most important factor affecting the fluorescence of BLT, the emission spectra of BLT in phosphate buffer solutions which contained different inorganic salts, amino acid and reactive oxygen species was recorded, including SDS, $MgCl_2$, NaCl, NaAc, KCl, Hcy, Cys, H_2O_2, ClO^-, $ONOO^-$. The control group was measured in phosphate buffer solution at pH 7.4 without adding any other species. SDS is an anionic surfactant, which can lower the local pH of the solution and act as a hydrogen ion response group [33]. As depicted in Fig. 2C, among various tested species, only BLT with the addition of SDS showed a distinguished fluorescence intensity ratio (I_{670}/I_{610}) increase, suggesting that other tested species unable to cause changes in fluorescence of BLT and BLT possess highly selective to pH. In view of the above spectral results, the response mechanism of BLT to H^+ are shown in Fig. 2D. In acidic medium,

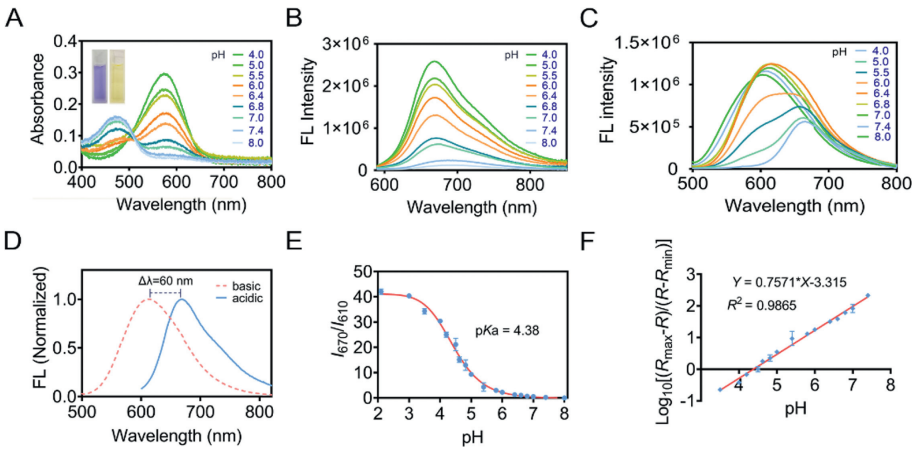

Fig. 1. (A) Absorption spectra of BLT (10 μmol/L) at phosphate buffer solutions with various pH (1% DMSO), the insert shows the colors of BLT in phosphate buffer solutions at pH 4 (left) and pH 8 (right). (B) Fluorescence spectra of BLT at phosphate buffer solutions with various pH (λ_{ex} = 580 nm). (C) Fluorescence spectra of BLT at phosphate buffer solutions with various pH (λ_{ex} = 480 nm). (D) Fluorescence spectra of BLT at acidic and basic conditions. (E) Plot of fluorescence intensity ratio (I_{670}/I_{610}) *versus* pH for BLT. (F) The plot of $\log_{10}[(R_{max} - R)/(R - R_{min})]$ *versus* pH. R is the ratio of fluorescence intensity (I_{670}/I_{610}).

the N atom in the quinoline ring of BLT was protonated, which in turn changed the π-electron conjugate system. The color of BLT solution also transformed and got purple, which can be clearly seen from Fig. 2D. To further verify BLT response mechanism, ^{1}H NMR titration analysis of BLT using HCl in DMSO-d_6 was conducted. With the addition of HCl, the protonation of the N atom on the quinoline ring was formed and triggered π-electron rearrangement, which promoted downfield shifts of the H1, H2 and upfield shifts of the H3 in BLT (Fig. 2E). At the same time, it could be obvious seen that there was an extra proton peak at the chemical shift 10.39 ppm, which was assigned to the H4' proton on the nitrogen atom of the previous quinoline ring. Moreover, the density functional theory (DFT) calculations of BLT were performed to study the extraordinary shifts in absorption and emission spectra of neutral form and ionic form by using the B3LYP 6-31G* level. As depicted in Fig. S6 (Supporting information), the calculated energy gap (HOMO-LUMO) of the ionic form of BLT is smaller than that of neutral form, 2.600 eV and 2.948 eV, respectively, which theoretically verified that the neutral from is transformed into ionic form with spectral red shift.

Next, cytotoxicity of BLT was evaluated by MTT method, in which MCF-7 (human breast cancer cells), U87 (human glioma cells) and L02 (human hepatocytes) were performed. BLT did not show any conspicuous cytotoxicity at different concentrations (Fig. S7 in Supporting information). Then, the ability of BLT co-localization with lysosomes was examined using LysoTracker Blue. As depicted in Figs. S8A and B (Supporting information), BLT exhibited fluorescence signals in the green channel (λ_{ex} = 488 nm), and the red channel also emitted fluorescence (λ_{ex} = 543 nm), indicating that BLT can enter the cell membrane as a neutral form and be converted into an ionic form to reside in the cell. Moreover, the red fluorescence of BLT (λ_{ex} = 543 nm) completely overlaps with the blue fluorescence of LysoTracker Blue. As depicted in Figs. S8C and D (Supporting information), the corresponding overlap coefficient (OLC) and Pearson's correlation coefficient (PCC) of BLT (λ_{ex} = 543 nm) with LysoTracker Blue were 0.90 and 0.92 for MCF-7 cells, and 0.90 and 0.91 for U87cells, respectively. Based on the above-mentioned imaging finds, it can be indicated that the fluorescence of BLT (λ_{ex} = 543 nm) seemed that BLT can accumulate in lysosomes with high selectivity.

Subsequently, whether BLT detected pH alters in living cells was tested. Cells were stained with BLT in PBS containing 10 μmol/L of nigericin at various pH values. Nigericin which is an H^+/K^+ ionophore, can balanced the lysosomal internal and surrounding pH [26,34]. As represented in Fig. 3A, the green fluorescence grew stronger (λ_{ex} = 488 nm) and the red fluorescence gain weaker in MCF cells (λ_{ex} = 543 nm), with the pH of the incubation increased. At the same time, the dramatic color of the two-overlay channels varied from bright orange to yellowish green. As the pH increased, the ratio (I_{red}/I_{green}) gradually decreased (Fig. 3B). In addition, similar results were observed for U87 cells (Fig. S9 in Supporting information). These results indicated that BLT possessed the characteristic of monitoring alters of lysosomal pH value in living cells.

Furthermore, BLT was applied to observe alters in lysosomal acidity of cells under heat stress. As revealed in Fig. S10A (Supporting information), MCF-7 cells were stained by BLT at 37, 41 and 45 °C. 41 and 45 °C served as the heat stress group. Compared with group at 37 °C, the green fluorescence weakly increased at 41 and 45 °C, and accompanied by the red fluorescence channel decreased. Moreover, although the fluorescence change of the individual channels is not particularly obvious, the color of the two-overlay channel changed from orange to yellow-green (Fig. S10A). The fluorescence intensity ratios (I_{red}/I_{green}) exhibited a temperature-dependent feature (Fig. S10C in Supporting information). With the culture environment temperature rises to 45 °C, I_{red}/I_{green} gradually decreases. Similar experiments were implemented for U87 cells (Fig. S10B in Supporting information) and the phenomenon was the same as MCF-7 cells. All above results revealed that pH of lysosome rose after cells undergoes heat stress.

Next, whether BLT can detect lysosomal pH changes under oxidative stress was investigated. Oxidative stress inducer H_2O_2 can redistribute H^+ to the cytoplasmic compartment from acidic compartments by damaging vacuolar proton pump, and this process requires ATP consumption to import H^+. Oxidation stress lysosome alkalization and cytoplasmic acidification have also been reported in some literatures [35]. As depicted in Fig. 3C, compared to the normal group, the green fluorescence in the cells pretreated with H_2O_2 increased while the red fluorescence decreased. Moreover, I_{red}/I_{green} was lower than that of normal group (Fig. 3D). Together, the present findings confirmed that the pH of lysosomes increased under cell oxidative stress.

Subsequently, we wondered whether the drug-induced injury stress would affect the pH of the lysosome in live cell. Overdose APAP induces acute liver injury has been confirmed in some literature [30]. As depicted in Fig. 3C, compared to normal group, the green fluorescence of cells after APAP-induced stimulation raised while the red fluorescence decreased. Moreover, the color of the two-overlay channel changed from orange to yellow, which was

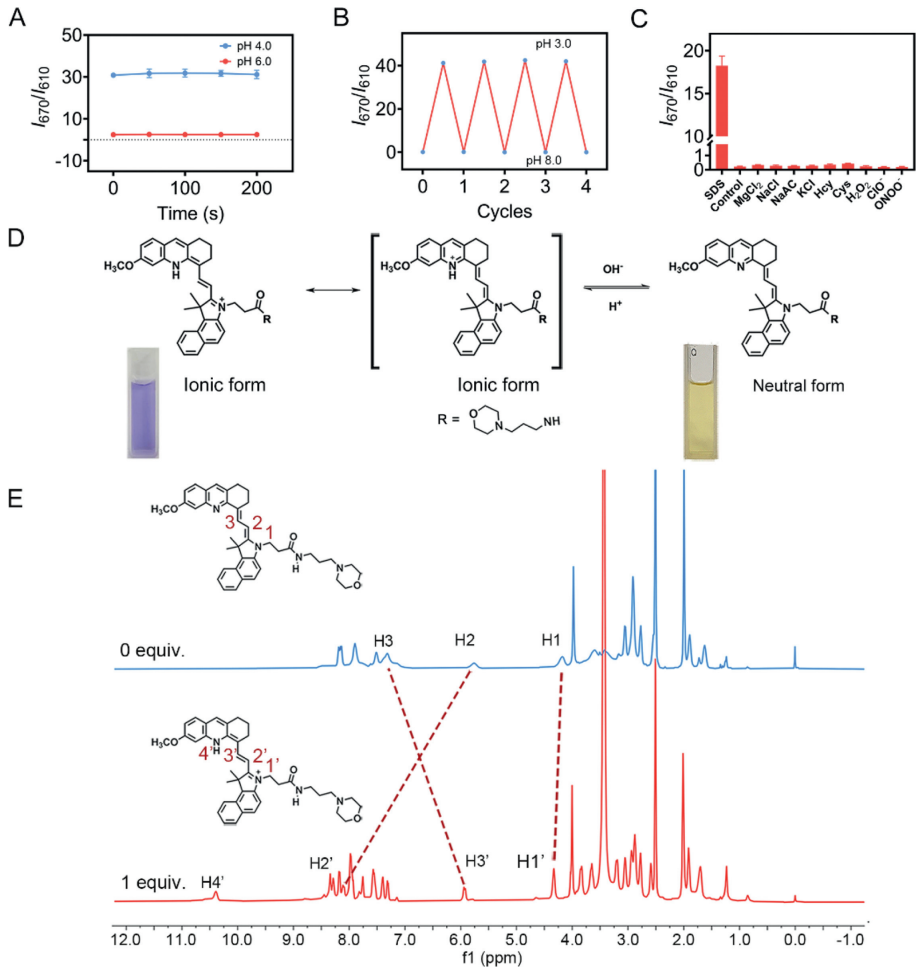

Fig. 2. (A) The fluorescence intensity ratio (I_{670}/I_{610}) of BLT (10 μmol/L) changes over time in phosphate buffer solutions with pH 4 and 6. (B) The fluorescence intensity ratios I_{670}/I_{610} of BLT (10 μmol/L) to various interferents (10 mmol/L for inorganic salts, amino acid; 50 μmol/L for H_2O_2, ClO^-, $ONOO^-$) in phosphate buffer solution at pH 7.4. (C) pH reversibility of BLT in PBS buffer solution (pH = 3 and 8). (D) Structural interconversion between the ionic and neutral forms of fluorophore BLT. (E) ^1H NMR titration spectra of BLT with 0 equiv. of HCl and 1 equiv. of HCl in DMSO-d_6.

more intuitive than the change of the fluorescence intensity of the single channel. The ratios I_{red}/I_{green} of APAP-induced injury group displayed decrease (Fig. 3D). The reason for this phenomenon can be speculated that the permeability of the lysosomal membrane changes after cell treated with APAP, which leads to the leakage of hydrogen ions in the lysosome. These results demonstrated that BLT can monitor the changes in lysosomal pH under cell APAP-induced injury.

After achieving live cell imaging with BLT, whether BLT can track the change of lysosomal pH in liver tissue injury model was further explored, the liver tissue of mice induced by APAP was stained with BLT. First, we explored whether the probe can co-localize with lysosomes on liver tissue. As shown in Figs. S11A and B (Supporting information), the fluorescence of BLT and commercial lysosomal probes LysoTracker Blue on liver tissue sections had a good overlap. Three-dimensional (3D) reconstructed images of liver tissues displayed the distribution of lysosomes on the tissue, as is revealed in Fig. S11C (Supporting information), lysosomal blue fluorescence is almost the same as the red fluorescence of BLT for spatial distribution. It shows that BLT can also stain well with lysosomes on liver tissue. After that, as shown in Fig. 4A, we constructed an APAP-induced liver injury mouse model. Histological analysis of liver tissue was implemented. Compared with saline group, moderate edema of hepatocytes was found in the liver tissues in APAP-induced group (Fig. 4B). This hinted that APAP can cause liver toxicity in mice. At the same time, green fluorescence increased on APAP-induced liver tissue group while red fluorescence decreased, which can also be observed from the relative fluorescence intensity (Fig. 4C). The ratios (I_{red}/I_{green}) of APAP-induced injury group exhibited decline (Fig. 4D). Those above results indicated that BLT can track the increase of lysosomal pH in the liver tissue of APAP-induced liver injury mice. The results of experiment found clear support for that BLT possesses potential functions in investigating the physiological processes related to drug-induced hepatotoxicity.

Finally, inspired by the outstanding fluorescence characteristics of the probe from the above results, the pH variations of lysosomes in live zebrafish by APAP-stimulated were also monitored by BLT. The zebrafish were divided into two groups, one of which is the control group, cultured in normal medium, and the other is the APAP-induced injury group (Fig. 5A). As depicted in Fig. 5B, the zebrafish stimulated by APAP and BLT revealed brighter green fluorescence intensity and lower red fluorescence intensity at liver area and the color of the merge channel changed from yellow to greenish-yellow clearly, which were shown in the enlarged area. The relative fluorescence intensity of the image also exhibited same conclusion (Fig. 5C). Moreover, the ratio (I_{red}/I_{green}) in APAP-induced injury group showed a downward trend (Fig. 5D). These results indicated that the pH of the lysosome in zebrafish liver has increased. It can be anticipated that lysosomal-targeting and ratio-

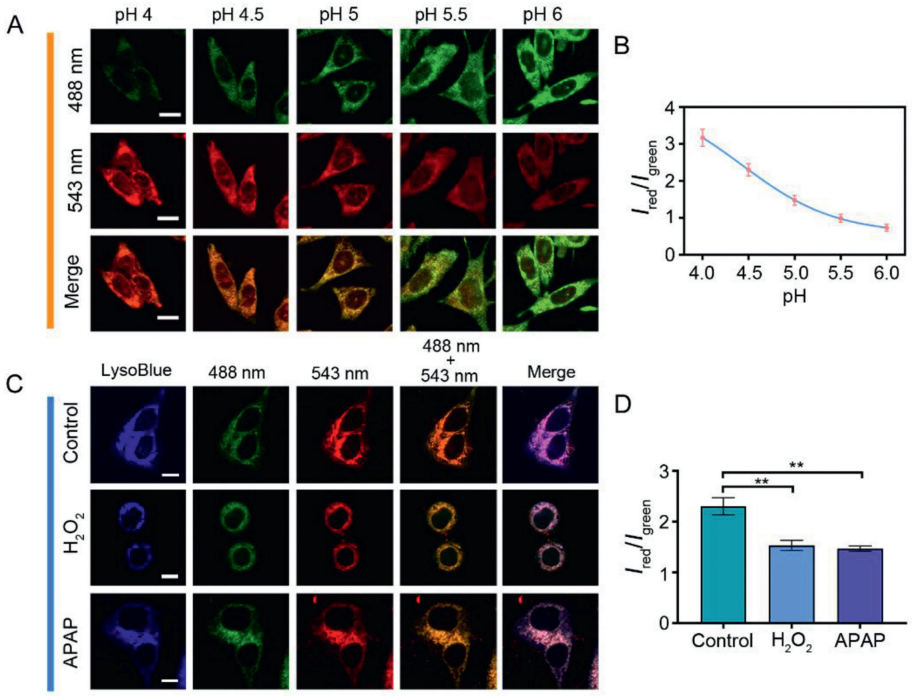

Fig. 3. (A) Fluorescence imaging of MCF-7 cells cultured with BLT (10 μmol/L, λ_{ex}, 488 nm and 543 nm) at various pH. (B) The fluorescence intensity ratios (I_{red}/I_{green}) at various pH in MCF-7. (C) Fluorescence imaging of L02 cells cultured with BLT (10 μmol/L, λ_{ex}, 488 nm and 543 nm) under oxidative stress and APAP-induced injury stress. (D) The fluorescence intensity ratios (I_{red}/I_{green}) under different stress conditions in L02 cells. Scar bar: 10 μm. The statistical differences were conducted *via* Student's *t*-test. ** $P < 0.01$.

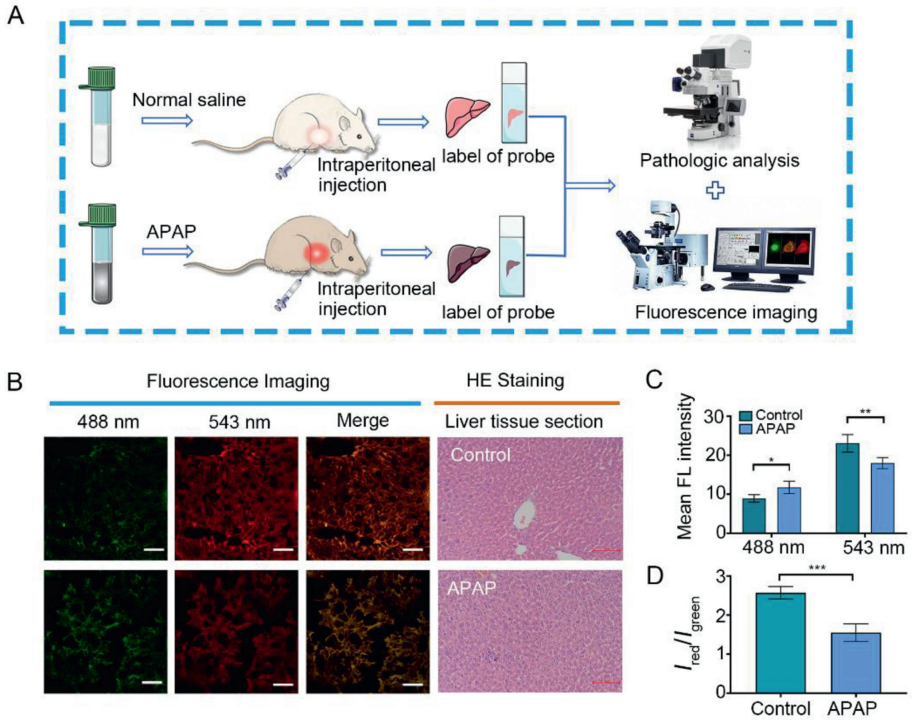

Fig. 4. (A) Schematic diagram of experiment model in mice. (B) Fluorescence imaging and hematoxylin-eosin staining of liver tissues stimulated by saline or APAP (300 mg/kg, intraperitoneally) stained with BLT (50 μmol/L, λ_{ex}, 488 nm and 543 nm). (C) The relative fluorescent intensities of liver tissues stimulated by saline or APAP. (D) The fluorescence intensity ratios (I_{red}/I_{green}) of liver tissues. Scale bar: 100 μm. The statistical differences were conducted *via* Student's *t*-test. * $P < 0.05$; ** $P < 0.01$; *** $P < 0.001$.

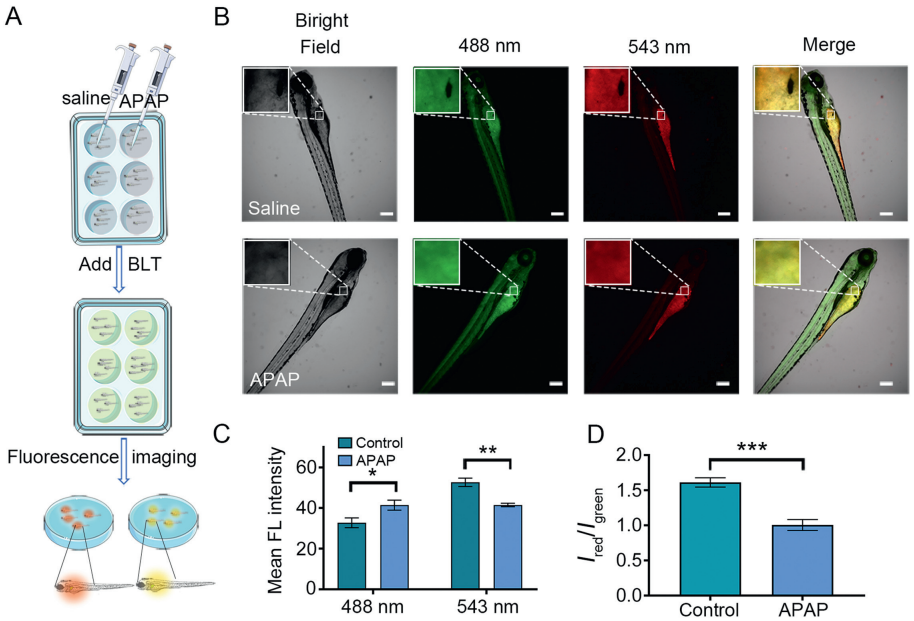

Fig. 5. (A) Fluorescence imaging of zebrafish stimulated by saline or APAP (1000 μmol/L) stained with BLT (20 μmol/L, λ_{ex}, 488 nm and 543 nm). (B) The relative fluorescent intensities of zebrafish stimulated by saline or APAP. (C) The fluorescence intensity ratios (I_{red}/I_{green}) of zebrafish. (D) Schematic diagram of zebrafish experiment model. Scale bar: 100 μm. The statistical differences were conducted via Student's *t*-test. * $P < 0.05$; ** $P < 0.01$; *** $P < 0.001$.

metric probe displays good performance in the investigations on pH-relevant biological processes.

In conclusion, a NIR ratiometric pH-responsive fluorescent probe with hemicyanine skeleton was developed. This probe exhibited excellent ratiometric pH sensitivity characteristics with a suitable pK_a for lysosomes and good targeting ability to lysosomes. Importantly, BLT possessed considerable value for investigating lysosomal pH varieties associated with heat stress, oxidative stress or drug-induced injury. This ratiometric fluorescent probe innovatively tracks changes in lysosomal pH in APAP-induced liver injury in live cells, mice, and zebrafish. Moreover, we anticipate that this development of novel fluorescent probes fluorescent probe may contribute a new idea for exploring lysosomal-associated physiological varieties of drug-induced hepatotoxicity.

Ethics statement

All animal experiments were performed according to the ethical policies and regulations provided by Guide for the Care and Use of Laboratory Animals (National Institutes of Health).

Declaration of competing interest

The authors declare that they have no known competing financial interests or personal relationships that could have appeared to influence the work reported in this paper.

Acknowledgments

The authors are grateful to the Natural Science Foundation of China (NSFC, No. 82001981), the fifth phase of "333 High-level Talent Cultivation Project" in Jiangsu Province (No. 1092000102) and the Fundamental Research Funds for the Central Universities (No. 2632022ZD01).

Supplementary materials

Supplementary material associated with this article can be found, in the online version, at doi:10.1016/j.cclet.2022.06.009.

References

[1] S. Fulda, A.M. Gorman, O. Hori, A. Samali, Int. J. Cell. Biol. (2010) 214074.
[2] Y. Ishida, S. Nayak, J.A. Mindell, et al., J. Gen. Physiol. 141 (2013) 705–720.
[3] G.H. Sun-Wada, Y. Wada, M. Futai, Biochim. Biophys. Acta 1658 (2004) 106–114.
[4] J.R. Casey, S. Grinstein, J. Orlowski, Mol. Cell Biol. 11 (2010) 50–61.
[5] X. Liu, Y. Su, H. Tian, et al., Anal. Chem. 89 (2017) 7038–7045.
[6] X. Shi, N. Yan, G. Niu, et al., Chem. Sci. 11 (2020) 3152–3163.
[7] R.E. Lawrence, R. Zoncu, Nat. Cell Biol. 21 (2019) 133–142.
[8] S.M. Davidson, M.G. Vander Heiden, Annu. Rev. Pharmacool. Toxicol. 57 (2017) 481–507.
[9] H. Hou, Y. Zhao, C. Li, et al., Sci. Rep. 7 (2017) 1759.
[10] B.A. Webb, M. Chimenti, M.P. Jacobson, et al., Nat. Rev. Cancer 11 (2011) 671–677.
[11] G. Kroemer, M. Jäättelä, Nat. Rev. Cancer 5 (2005) 886–897.
[12] J. Han, K. Burgess, Chem. Rev. 110 (2010) 2709–2728.
[13] Y. Sun, X. Zhou, L. Sun, et al., Chin. Chem. Lett. 33 (2022) 4229–4232.
[14] Z. Yuan, J. Chen, Q. Zhou, et al., Chin. Chem. Lett. 32 (2021) 1803–1808.
[15] H. Ogasawara, Y. Tanaka, M. Taki, S. Yamaguchi, Chem. Sci. 12 (2021) 7902–7907.
[16] E.A. Owens, M. Henary, G. El Fakhri, et al., Acc. Chem. Res. 49 (2016) 1731–1740.
[17] C. Staudinger, S.M. Borisov, Methods Appl. Fluoresc. 3 (2015) 042005.
[18] G. Niu, P. Zhang, W. Liu, et al., Anal. Chem. 89 (2017) 1922–1929.
[19] S.I. Reja, M. Minoshima, Y. Hori, et al., Chem. Sci. 12 (2020) 3437–3447.
[20] L. Yuan, W. Lin, S. Zhao, et al., J. Am. Chem. Soc. 134 (2012) 13510–13523.
[21] Q. Xia, S. Feng, J. Hong, et al., Talanta 228 (2021) 122184.
[22] T. Zhang, F. Huo, W. Zhang, et al., Sens. Actuat. B: Chem. 345 (2021) 130393.
[23] P. Ning, L. Hou, Y. Feng, et al., Chem. Commun. 55 (2019) 1782–1785.
[24] J. Ge, L. Fan, K. Zhang, et al., Sens. Actuat. B: Chem. 262 (2018) 913–921.
[25] G. Song, D. Jiang, L. Wang, et al., Chin. Chem. Lett. 33 (2022) 339–343.
[26] Q. Wan, S. Chen, W. Shi, et al., Angew. Chem. Int. Ed. 53 (2014) 10916–10920.
[27] H. Zhu, J. Fan, Q. Xu, et al., Chem. Commun. 48 (2012) 11766–11768.
[28] X. Chen, Q. Chen, M. Chen, et al., Sens. Actuators B: Chem. 329 (2021) 129104.
[29] G.-J. Mao, Z.-Z. Liang, G.-Q. Gao, et al., Anal. Chim. Acta 1092 (2019) 117–125.
[30] D. Cheng, J. Peng, Y. Lv, et al., J. Am. Chem. Soc. 141 (2019) 6352–6363.
[31] D. Cheng, W. Xu, L. Yuan, et al., Anal. Chem. 89 (2017) 7693–7700.
[32] Y. Li, X. Xie, X.e. Yang, et al., Chem. Sci. 8 (2017) 4006–4011.
[33] Y. Liu, J. Zhou, L. Wang, et al., J. Am. Chem. Soc. 138 (2016) 12368–12374.
[34] Y. Yue, F. Huo, X. Li, et al., Org. Lett. 19 (2017) 82–85.
[35] M.H. Lee, J.H. Han, J.H. Lee, et al., Angew. Chem. Int. Ed. 52 (2013) 6206–6209.